EPiC Series in Computing

Volume 104, 2024, Pages 25–35

Proceedings of 3rd International Workshop on
Mathematical Modeling and Scientific Computing

Development of Numerical Algorithms for Multicontact Problems of Mechanics Considering Various Inelastic Effects

Pavel S. Aronov[1,2], Mikhail P. Galanin[1,2], and Alexandr S. Rodin[1,2]

[1] Keldysh Institute of Applied Mathematics RAS, Moscow, Russia
[2] Bauman Moscow State Technical University, Moscow, Russia
aronovps@mail.ru
galan@keldysh.ru
rals@bk.ru

Abstract

Algorithms for the numerical solution of contact quasi-static problems of deformable solid mechanics were constructed. The contact interaction of the body system was considered using the mortar method (a variant of the Lagrange multiplier method). The developed algorithms were used to simulate the thermomechanical state of a fuel element section, considering creep and cracking. The results of calculations for axisymmetric formulation of the problem for the operation mode of a fuel element with constant heat release in fuel pellets are presented.

1 Introduction

The assessment of the equipment critical components reliability and durability is based on an analysis of the structure stress-strain state, considering the contact interaction features. There is no analytical solution for most practically important contact problems, therefore numerical methods are used to determine the displacement and stress fields. Among them, the following can be noted: the domain decomposition method [16, 6], the penalty method [4, 11], various variants of the Lagrange multiplier method [19], in particular, the mortar method [17], which offers a great facility for coupling different variational approximations and therefore using mismatched grids at the subdomains interfaces.

The paper presents a general formulation of the quasi-static multicontact problem and introduces the algorithm for the numerical solution of such problems, considering cracking and creep. The mortar method was used to ensure that the boundary conditions were met on the contact surfaces between the bodies.

This article continues a series of publications devoted to modeling various thermomechanical processes in a fuel element section: in [1], a demonstration multicontact problem is solved in a thermoelastic approximation. In [2], the creep effect was added to the material model, and a section of fuel rod containing from 1 to 100 pellets was modeled. In this work, an account of the

V.L. Turova, A.E. Kovtanyuk and J. Zimmer (eds.), MMSC 2024 (EPiC Series in Computing, vol. 104), pp. 25–35

cracking of fuel pellets has been added, which is performed using the smeared crack model [5], and the presence of a gap between the pellets and the cladding is also considered. This model boils down to the fact that during the loading of a material, its elastic properties change, and in different directions these changes occur unevenly. Thus, after considering cracking, it is necessary to solve the creep problem for a material with anisotropic elastic properties.

In addition to using the mortar method to simulate the contact interaction of fuel elements, the authors also used variants of the domain decomposition method (DDM). These methods make it possible to reduce the solution of a global problem for a system of bodies to solving a number of local problems for each body separately within the framework of an iterative process. In this case, either kinematic (analogous to the Dirichlet condition) or force (Neumann condition) boundary conditions are set on each contact surface. The effectiveness of the DDM methods is determined by the convergence rate of the corresponding iterative process. In [8], the rate of convergence of iterations in the Neumann — Dirichlet method for the problem of modeling a fuel element section comprising from 1 to 100 fuel pellets in a thermoelastic axisymmetric formulation is investigated. The paper [7] presents the results of solving a similar problem in a three-dimensional formulation (for the sector 90°). In [9], an axisymmetric problem is examined for a section of 10 pellets, considering cracking for pellets and the formation of plastic deformations for the cladding, and in the thermal problem, the condition of ideal thermal contact is set on the contacting surfaces.

2 Mathematical formulation of the problem

Consider that in the three-dimensional space $\mathbb{R}^3$ there is a group of contacting bodies occupying the area $G = \bigcup\limits_{\alpha=1}^{N} G_\alpha$ (α — index denoting the body number), bounded by a piecewise smooth boundary $\partial G = \bigcup\limits_{\alpha=1}^{N} \partial G_\alpha$.

Consider the following problem simulating some processes taking place in a fuel rod: inside the cylindrical cladding G_N there is a column of several identical cylindrical pellets $G_1, \ldots, G_{N-1}$ stacked on top of each other, having an inner hole and chamfers at both ends.

We assume that the cladding temperature is constant, and to find the temperature in the fuel pellets, the following initial boundary value problem is solved for the thermal conductivity equation in the region $G_p = G \backslash G_N$ [20]:

$$c(T)\rho\frac{\partial T}{\partial t} = (k_{ij}(T)T_{,j})_{,i} + q(\mathbf{x},t), \quad \mathbf{x} \in G_p, \quad t > 0; \tag{1}$$

$$T(\mathbf{x},0) = T_0(\mathbf{x}), \quad \mathbf{x} \in G_p; \tag{2}$$

$$-n_i k_{ij}(T)T_{,j}\Big|_{\partial G_p} = 0, \quad \mathbf{x} \in \partial G_p \backslash S_{T3} \quad t > 0; \tag{3}$$

$$-n_i k_{ij}(T)T_{,j} = h[T(\mathbf{x},t) - T_{clad}], \quad \mathbf{x} \in S_{T3}, \quad t > 0, \tag{4}$$

where t is time, x_i are the coordinates of the vector $\mathbf{x} \in G_\alpha$, $T(\mathbf{x},t)$ is temperature at time t, $c(T)$ is specific heat capacity of the medium, ρ is density of the medium, k_{ij} are the components of the thermal conductivity tensor, $T_{,j} = \dfrac{\partial T}{\partial x_j}$, $q(\mathbf{x},t)$ is power of internal heat sources, $T_0(\mathbf{x})$ is initial temperature, n_i are the components of the external normal vector to the boundary ∂G, h is the coefficient of heat transfer on the surface S_{T3} (union of the outer surfaces of pellets),

on which the condition of heat exchange between pellets and the cladding is set, T_{clad} is the cladding temperature.

The mathematical formulation of the quasi-static thermomechanics problem, considering creep deformations, includes the following relations for each body α $(i, j = \overline{1,3})$ [20]:

- equilibrium equations
$$\sigma_{ji,j}(\mathbf{x}, t) = 0, \quad \mathbf{x} \in G_\alpha, \quad t > 0; \tag{5}$$
- kinematic boundary conditions
$$u_z(\mathbf{x}, t) = 0, \quad \mathbf{x} \in S_1, \quad t > 0; \tag{6}$$
- force boundary conditions
$$\sigma_{ji}(\mathbf{x}, t)n_j = g_i(\mathbf{x}, t), \quad x \in S_2, \quad t > 0; \tag{7}$$
- Cauchy relations for the linear full strain tensor
$$\varepsilon_{ij}(\mathbf{x}, t) = \frac{1}{2}(u_{i,j}(\mathbf{x}, t) + u_{j,i}(\mathbf{x}, t)), \quad \mathbf{x} \in G_\alpha, \quad t > 0; \tag{8}$$
- defining equations (Hooke's law)
$$d\sigma_{ij}(\mathbf{x}, t) = C_{ijkl}(T)\left(d\varepsilon_{kl}(\mathbf{x}, t) - d\varepsilon^T_{kl}(\mathbf{x}, t) - d\varepsilon^c_{kl}(\mathbf{x}, t)\right), \quad \mathbf{x} \in G_\alpha, \quad t > 0, \tag{9}$$

where x_i are the coordinates of the vector $\mathbf{x} \in G_\alpha$, u_i are the displacement vector components; σ_{ij} are the Cauchy stress tensor components; ε_{kl} are the full tensor deformations components; ε^T_{kl} are the temperature strain tensor components; ε^c_{kl} are the creep strain tensor components; C_{ijkl} are the elastic tensor constants components; g_i are the surface forces vector components.

The model considers that each pellet (except G_1 and G_{N-1}) comes into contact with two adjacent (top and bottom) pellets and the cladding.

Consider a pair of potentially contact surfaces related to bodies with numbers α_1 and α_2. To simplify the recording, we use the index '1' instead of 'α_1' and '2' instead of 'α_2'. Then the additional conditions on the S^1_k surface for the case of frictionless contact look like this (for the S^2_k surface the conditions are written similarly) [6, 19]:

$$\sigma^1_\tau(\mathbf{x}, t) = \sigma^2_\tau(\bar{\mathbf{x}}, t) = 0, \tag{10}$$
$$\sigma^1_n(\mathbf{x}, t) = \sigma^2_n(\bar{\mathbf{x}}, t) \leqslant 0, \tag{11}$$
$$u^1_n(\mathbf{x}, t) + u^2_n(\bar{\mathbf{x}}, t) \leqslant \delta_{0n}(\mathbf{x}, t), \tag{12}$$
$$\sigma^1_n(\mathbf{x}, t)\left(u^1_n(\mathbf{x}, t) + u^2_n(\bar{\mathbf{x}}, t) - \delta_{0n}(\mathbf{x}, t)\right) = 0. \tag{13}$$

Here $\mathbf{x}$ is some point lying on the S^1_k surface, $\bar{\mathbf{x}}$ is a similar point located opposite it on the S^2_k surface, $\delta_{0n}(\mathbf{x}, t) \geqslant 0$ is the initial gap function (the surface sections could not touch each other at the initial moment), $u^\alpha_n = \mathbf{u}^\alpha \cdot \mathbf{n}^\alpha$, $\sigma^\alpha_\tau = (\sigma^\alpha \cdot \mathbf{n}^\alpha) \cdot \tau^\alpha$, $\sigma^\alpha_n = (\sigma^\alpha \cdot \mathbf{n}^\alpha) \cdot \mathbf{n}^\alpha$, $\alpha = 1, 2$ (summation by α is not performed).

The conditions (10)–(13) guarantee that on some S^{12}_k section S^1_k and S^2_k surfaces will coincide (the configuration and position of this section are unknown in advance), in this case, compressive contact forces will act on the contacting bodies. In the considered system, the set of contact surfaces S_k includes $N - 2$ pellet/pellet contact pairs and $N - 1$ pellet/cladding contact pairs.

To model the creep process, the flow theory is used, the main provisions of which include [13]:

- additive decomposition of the full strain tensor time derivative

$$d\varepsilon_{ij} = d\varepsilon^e_{ij} + d\varepsilon^c_{ij} + d\varepsilon^T_{ij}; \tag{14}$$

- incompressibility of creep deformation

$$d\varepsilon^c_{ii} = 0; \tag{15}$$

- relation for the creep strain tensor time derivative

$$\dot{\varepsilon}^c_{ij} = \dot{\mu}\sigma'_{ij}, \tag{16}$$

where $\dot{\mu} = \frac{3}{2}\frac{\dot{\varepsilon}^c_i}{\sigma_i}$, $\sigma_i = \sqrt{\frac{3}{2}\sigma'_{kl}\sigma'_{kl}}$ is stress intensity, $\dot{\varepsilon}^c_i = f(T, \sigma_i)$ is the dependence for creep strain rate, $\sigma'_{kl} = \sigma_{kl} - \frac{1}{3}\sigma_{mm}\delta_{kl}$.

To consider pellets cracking, the smeared crack model is applied, in which it is assumed that the increment of elastic deformation is associated with the increment of stresses by the following equation [15]

$$d\varepsilon^e_{ij} = \tilde{C}^{-1}_{ijkl} d\sigma_{kl}, \tag{17}$$

moreover, the coefficients of the compliance tensor $\tilde{C}^{-1}_{ijkl}$ depend on total deformations or total stresses (further in the article an example of a specific type $\tilde{C}^{-1}_{ijkl}$ is given).

Thus, the determining ratio in pellets can be written as

$$d\sigma_{ij} = \tilde{C}_{ijkl}\left(d\varepsilon_{kl} - d\varepsilon^T_{kl} - d\varepsilon^c_{kl}\right). \tag{18}$$

To discretize the thermal conductivity problem (1)–(4) and the mechanics problem (5)–(18), the finite element method (FEM) is used, and an algorithm based on the mortar method is built to consider the contact interaction of bodies.

3 Using of mortar method for solving contact problems

There is no analytical solution for the problem under consideration, therefore it is necessary to use numerical methods. To do this, we move from the initial differential formulation to the weak one. This transition can be carried out in various ways. Here is a method based on considering the energy of a system of N deformable bodies, which at time t_m looks like this

$$\Pi(t_m) = \sum_{\alpha=1}^{N} \Pi_\alpha(t_m) + \Pi_c(t_m), \tag{19}$$

where

$$\Pi_\alpha(t_m) = \frac{1}{2}\int\limits_{G_\alpha} \sigma^T(\varepsilon - \varepsilon^0)\, dG - \int\limits_{S_2} \mathbf{u}^T\mathbf{g}\, dS, \tag{20}$$

and Π_c is responsible for the contribution to the potential energy of distributed contact forces that act on the surfaces of contacting bodies; its specific type depends on the method used, among which one can distinguish the classical and augmented Lagrange multiplier methods, the penalty method, a combination of the Lagrange multiplier method and the penalty method,

Neumann — Dirichlet methods, Nietzsche's method, barrier function method, various combinations of barrier function method and penalty method, and others [18].

The paper uses the Lagrange multiplier method, for which Π_c looks like this:

$$\Pi_c(t_m) = \int\limits_{S_k} \left(\lambda_n(\mathbf{x}, t_m) g_n(\mathbf{x}, t_m) + \lambda_\tau(\mathbf{x}, t_m) g_\tau(\mathbf{x}, t_m)\right) dS, \tag{21}$$

where $g_n = (\mathbf{u^2} - \mathbf{u^1}) \cdot \mathbf{n}$, $g_\tau = (\mathbf{u^2} - \mathbf{u^1}) \cdot \boldsymbol{\tau}$ are gap functions (in the three-dimensional case, we need to consider the tangent plane, the function g_τ will be vector). If the friction-free sliding condition is set on the contact surfaces, then $\lambda_\tau = 0$.

Solving the problem (5)–(13) at time t_m is equivalent to minimizing the functional [14]

$$\Pi = \frac{1}{2} \int\limits_G \boldsymbol{\sigma}^T \boldsymbol{\varepsilon}\, dG - \int\limits_{S_2} \mathbf{u}^T \mathbf{g}\, dS + \int\limits_{S_k} \lambda_n \left(u_{2n}(\mathbf{x}) + u_{1n}(\mathbf{x}) - \delta_{0n}(\mathbf{x})\right) dS \tag{22}$$

when the kinematic boundary conditions (6) are met, where λ_n are Lagrange multipliers that are projections of stress vectors to the directions of external normals, $u_n = u_r n_r + u_z n_z$.

Minimizing the functional (22), which includes the integral over the contact surface, leads to the formation of the following system of linear algebraic equations with respect to the increment vectors over time $\Delta t = t_m - t_{m-1}$ [19, 12]:

$$\begin{bmatrix} K & M \\ M^T & 0 \end{bmatrix} \begin{Bmatrix} \Delta U \\ \Delta \lambda \end{Bmatrix} = \begin{Bmatrix} \hat{R}_u \\ \hat{R}_\lambda \end{Bmatrix}, \tag{23}$$

where

$$\left\{\hat{R}_u\right\} = \left\{\hat{R}\right\} - \left\{\hat{F}\right\} - \{\lambda\}^T [M]^T, \tag{24}$$

$$\left\{\hat{R}_\lambda\right\} = \{\hat{R}_\delta\} - [M]^T \{U\}, \tag{25}$$

$\{\Delta U\}$ is the nodal displacement increments vector, $\{\Delta\lambda\}$ is the Lagrange multiplier increments vector, $[K]$ is stiffness matrix, $\left\{\hat{R}\right\}$ is the external forces vector, $\left\{\hat{F}\right\}$ is the internal forces vector, $[M]$ is a matrix describing the interaction of various bodies with each other, $\{\hat{R}_\delta\}$ is a vector considering the presence of an initial gap between the contacting surfaces.

The algorithm, some features of the mortar method application in relation to the problem under consideration, as well as specific expressions for the introduced matrices and vectors are described in [1, 2].

Since the configuration of the contact surfaces is unknown in advance, a cycle of external iterations is carried out to account for its changes. On the outer iteration with the number $(i+1)$ $(i = 0, 1, 2\ldots)$ a mortar grid is used (and the matrix M formed on its basis), referring to an already known configuration from the previous i-th iteration.

If the increment of inelastic deformations $\left\{\Delta\varepsilon^0\right\}$ depends on the current values of deformations and stresses (creep or cracking considering), then even for a fixed contact configuration, the system of equations (23) is nonlinear and needs to be linearized with using one of the iterative methods (we talk about the cycle of internal iterations).

In the problem under consideration, it can be assumed that the vector of inelastic deformations includes temperature deformations and creep deformations ($\left\{\Delta\varepsilon^0\right\} = \left\{\Delta\varepsilon^T\right\} + \{\Delta\varepsilon^c\}$). For the cladding, the matrix of elasticity coefficients $\left[\hat{D}\right]$ has the standard form [12],

and for fuel pellets, when using the smeared crack model, the matrix $\left[\hat{D}\right]$ considering the cracking of the material and is set as follows [15]

$$\left[\hat{D}\right]^{-1} = \begin{bmatrix} 1/\hat{E}_r & -\nu/E & -\nu/E & 0 \\ -\nu/E & 1/\hat{E}_z & -\nu/E & 0 \\ -\nu/E & -\nu/E & 1/\hat{E}_\varphi & 0 \\ 0 & 0 & 0 & 1/G \end{bmatrix} \tag{26}$$

Here, the modified Young modules $\hat{E}_i$, depending on the current values of deformations ε_i $(i = r, \varphi, z)$, change from the nominal value of E (in the region of strong compression) up to a certain limit value of E_∞ (in the area of strong stretching). The calculations used the value $E_\infty = E/10$, and the arcctg function was used to set smooth transition between values.

Note that after the beginning of the cracking process, the pellet material acquires elastic anisotropy, this is considered when constructing a numerical algorithm for finding creep deformation.

If the simple iteration method is used for linearization, then by the $(i+1)$-th outer iteration and the $(s+1)$-th internal iteration needs to solve the following system of linear equations:

$$\begin{bmatrix} K^{(i,s)} & M^{(i)} \\ M^{(i)T} & 0 \end{bmatrix} \begin{Bmatrix} \Delta U^{(i+1,s+1)} \\ \Delta\lambda^{(i+1,s+1)} \end{Bmatrix} = \begin{Bmatrix} \hat{R}_u^{(i,s)} \\ \hat{R}_\lambda^{(i)} \end{Bmatrix}, \tag{27}$$

where the vector of increments of inelastic deformations $\left\{\Delta\varepsilon^{0\,(i,s)}\right\}^{(e)}$ is used to determine the local vectors of internal forces $\left\{\hat{F}^{(i,s)}\right\}^{(e)}$ (which makes up the global vector of internal forces $\left\{\hat{F}\right\}$ in the ratio (24)), and the matrices $\left[\hat{D}\right]$ set by (26) are used to determine the local stiffness matrices $\left[K^{(i,s)}\right]^{(e)}$ in the elements related to fuel pellets.

Consider the general situation when the simulated system includes N bodies and q pairs of contact surfaces. In this case, the matrices and vectors included in (27) allow the following block representation (omit the indexes responsible for iteration numbers) [3]:

$$[K] = \operatorname{diag}(K_1, \ldots, K_N), \quad [M] = [M_1, \ldots, M_N]^T, \tag{28}$$

$$\{\Delta U\} = \{\Delta U_1, \ldots, \Delta U_N\}^T, \quad \{\Delta\lambda\} = \{\Delta\lambda_1, \ldots, \Delta\lambda_q\}^T, \tag{29}$$

where the stiffness matrices for the i-th body K_i have dimension $n_i \times n_i$, $i = 1, \ldots, N$ (n_i are the number of unknown displacements in the i-th body, $n = n_1 + \ldots + n_N$), matrices M_i have the dimension $n_i \times m$ ($m = m_1 + \ldots + m_q$ is the total number of unknown Lagrange multipliers).

For the numerical solution of the (27) system, the LU decomposition algorithm for sparse matrices was used, implemented as the SparseLU procedure from the Eigen library[1].

4 Results of numerical solution

To assess the effect of the initial gap between the pellets and the cladding on the final stress-strain state, a number of calculations were performed for the fuel element section, including 10 pellets ($N = 11$). Consider realistic material characteristics (zirconium alloy for the cladding and uranium dioxide for fuel pellets), procedures from the MATPRO library were used [10].

[1] https://eigen.tuxfamily.org

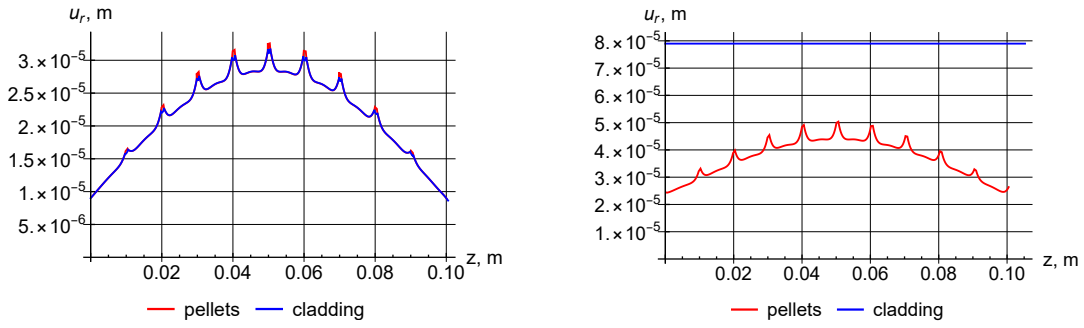

Figure 1: Graphs of radial displacements on the outer surface of the pellets and the inner surface of the cladding at a time of 1 year: (a) — calculation 1; (b) — calculation 3.

In the calculations performed, it was assumed that in the thermal problem $T_0 = 300$ K, $T_{clad} = 623$ K, the heat dissipation power is given by the function $q(\mathbf{x}, t) = q_0(t) \sin \dfrac{\pi z}{L}$, where L is the fuel column height, and $q_0(t)$ changes over time as follows: in 1 hour it increases linearly from 0 to the nominal value of q_{nom} and then remains constant. In the mechanical problem, the surface S_1, on which the kinematic conditions are set, includes the lower ends of the cladding and the lower pellet (they are fixed vertically), and the surface forces $g_i(\mathbf{x}, t)$ differ from zero only on the outer surface of the cladding (constant pressure 10 MPa) and on the upper end of the upper pellet (constant pressure 50 MPa).

The initial gap δ_{0n} between the pellets and the cladding in the calculation 1 was 0.01 mm, in the calculation 2 — 0.025 mm, in the calculation 3 — 0.06 mm. In all calculations, a time interval of 1 year was modeled (the typical operating time of the fuel element is several years).

A grid of second-order quadrangular finite elements is used in the calculations. After achieving the rated heat output power, the maximum temperature in the pellets reached a level of about 1500 K, due to heating, the fuel column shifted significantly relative to its initial position, while in the pellet/pellet contact pairs, most of the surface elements left contact (except for several elements located closer to the inner pellet surface). The development of creep deformations was considered only after the release of heat release in pellets at rated power (after 1 hour).

The graphs of stress and displacement distributions for various calculations are shown below, the stresses are given in MPa, and the displacements and coordinates are given in meters. The stress values are given in the Gauss points. To the values of radial displacements in the nodes corresponding to the surface of the cladding, the initial gap value is added.

Figure 1 shows graphs of radial displacements on the outer surface of pellets and the inner surface of the cladding for calculations 1 and 3 at the time of 1 year. As can be seen from the above graphs, in the case of a small gap (calculation 1, $\delta_{0n} = 0.01$ mm, Fig. 1(a)) all 10 pellets are in contact, the kinematic part of the contact conditions is fulfilled. If there is a sufficiently large gap between the pellets and the cladding (calculation 3, $\delta_{0n} = 0.06$ mm, Fig. 1(b)) there is no contact between the fuel column and the cladding.

Figure 2 shows graphs of radial displacements and stresses on the outer surface of the pellets and the inner surface of the cladding corresponding to calculation 2 at the time of 1 hour (Fig. 2(a) and Fig. 3(a)) and 1 year (Fig. 2(b) and Fig. 3(b)).

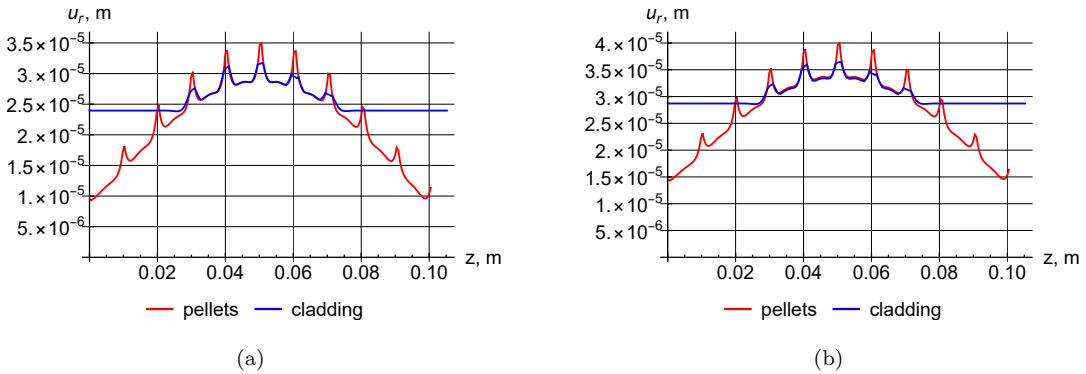

Figure 2: Graphs of radial displacements on the outer surface of the pellets and the inner surface of the cladding (calculation 2) at time: (a) — 1 hour; (b) — 1 year.

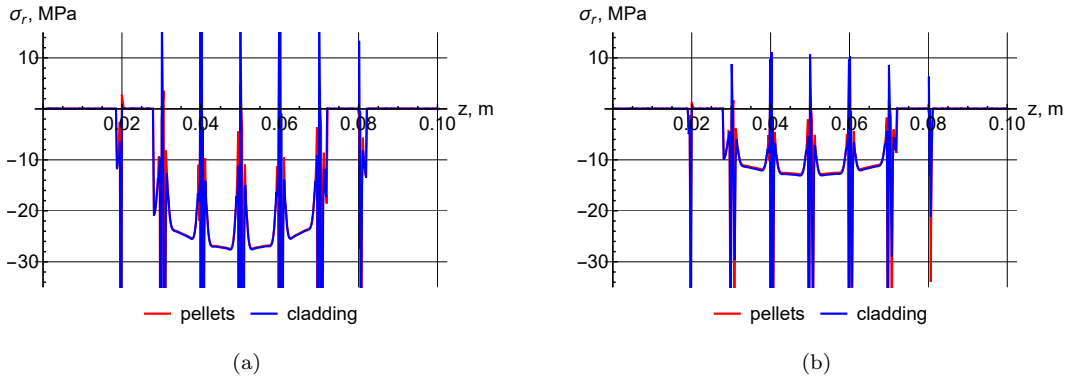

Figure 3: Graphs of radial stresses on the outer surface of the pellets and the inner surface of the cladding (calculation 2) at time: (a) — 1 hour; (b) — 1 year.

As can be seen from Fig. 2 and 3, if there is an initial gap $\delta_{0n} = 0.025$ mm, there are 4 pellets in contact with the cladding (from the 4th to the 7th), as well as small areas of the surfaces of the 3rd and 8th pellet. Graphs of radial displacements in Fig. 2 show the fulfillment of the kinematic part of the contact conditions (10)–(13), and the graphs of radial stresses in Fig. 3 show the fulfillment of the force part of the conditions in the pellet/cladding contact pairs for those surfaces that are in contact. The specified sinusoidal character of heat release leads to a sinusoidal distribution of contact forces and corresponding displacements and stresses along the fuel rod. Stress concentrators appear in the areas of the contact surfaces near the corners of the pellet facets. Considering the creep effect leads to a decrease in the level of radial stresses at the end of the calculation by 2.5 times compared to the time of 1 hour.

In Figures 4–5 graphs of the stress tensor components along the cross section drawn along the center of the 2nd pellet (not in contact, Fig. 4) and the 5th pellet (completely in contact, Fig. 5) at time points 1 hour and 1 year (the area corresponding to the coordinate $r > 0.0039$ m refers to the cladding). As can be seen from the figures, considering creep allows to reduce the level of tensile stresses several times. Comparison of Fig. 4(a) and 4(b), as well as Fig. 5(a) and 5(b)

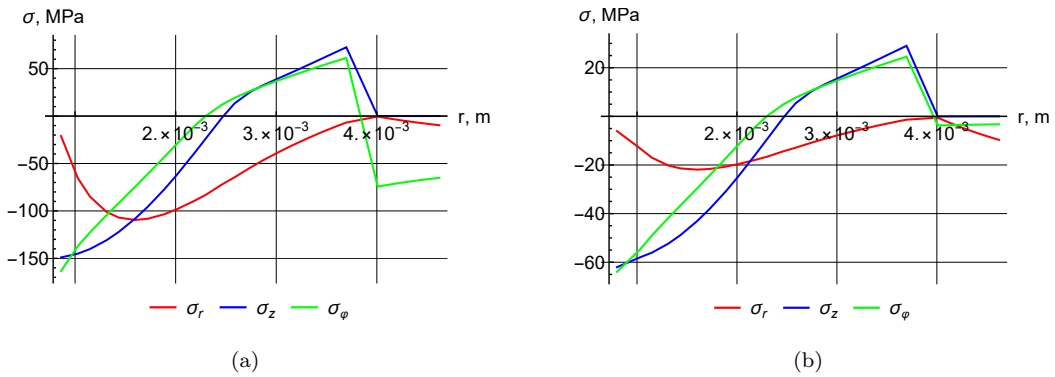

Figure 4: Graphs of radial stresses along the cross section of the 2nd pellet (calculation 2) at the time: (a) — 1 hour; (b) — 1 year.

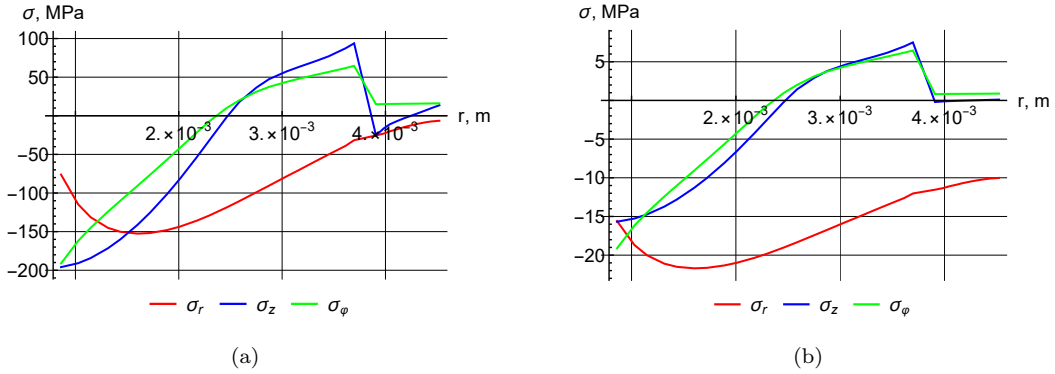

Figure 5: Graphs of radial stresses along the cross section of the 5th pellet (calculation 2) at the time: (a) — 1 hour; (b) — 1 year.

shows that the level of compressive stresses occurring in pellets closer to the inner surface is also significantly reduced. Considering cracking using the smeared crack model makes it possible to reduce the level of tensile stresses several times compared to the thermoelastic calculation (see, for example, [2]).

In Figure 6 graphs of radial displacements on the outer surface of pellets at the end of three calculations with different initial gaps are presented. These results demonstrate that with an increase in the initial gap, the values of radial displacements on the surface of the pellets also increase.

Figure 7 shows two-dimensional distributions of stress intensities at time points 1 hour and 1 year (calculation 2). Fragments of distributions related to the upper part of the 3rd pellet, the entire 4th pellet, the lower part of the 5th pellet and the corresponding portion of the cladding are shown, while when constructing deformed bodies, the applied displacements are increased 10 times for pellets and 50 times for the cladding for greater clarity.

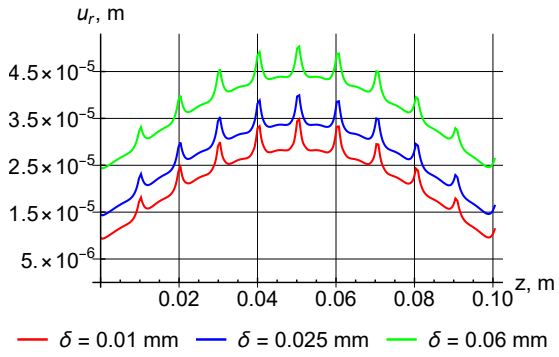

Figure 6: Graphs of radial displacements on the outer surface of pellets at $t = 1$ year for calculations 1, 2, 3.

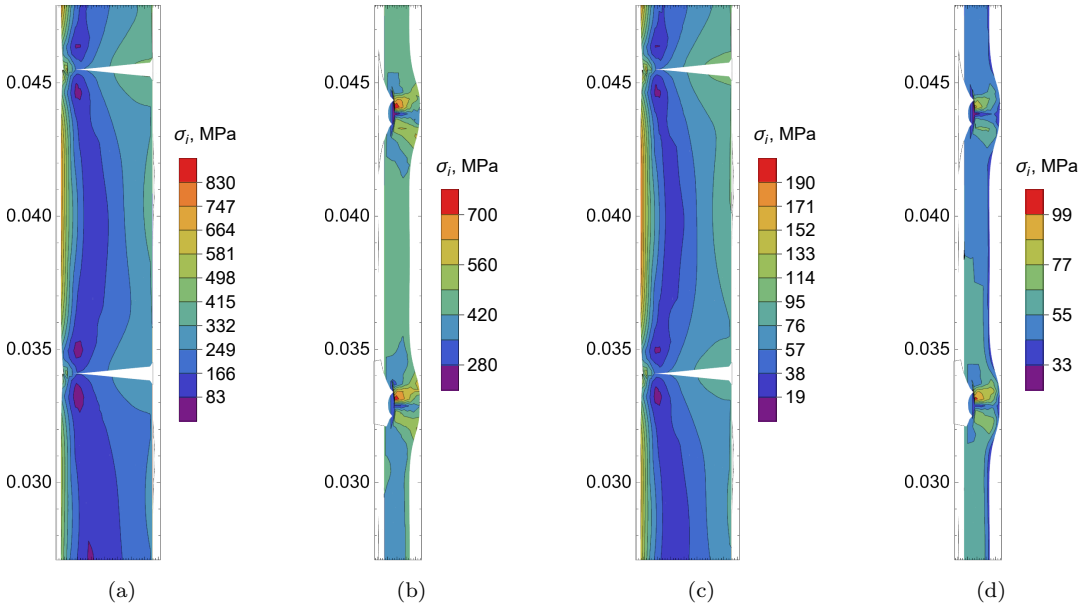

Figure 7: Two-dimensional stress intensity distributions, calculation 2: (a) — 1 hour (pellets); (b) — 1 hour (cladding); (c) — 1 year (pellets); (d) — 1 year (cladding).

5 Conclusion

The paper presents the formulation of a quasi-static problem of multicontact interaction of axisymmetric thermoelastic bodies under thermomechanical loading, considering the effects of cracking and creep. An algorithm for the numerical solution of such problems based on the finite element method is constructed. The mortar method was used to account for boundary conditions on contact surfaces. The results of applying the described algorithm to solve a demonstration problem simulating the thermomechanical state of a fuel element section including 10 fuel pellets for a mode with a given heat dissipation capacity, as well as the presence of an initial gap between the pellet and the cladding at a time interval of 1 year are shown.

Realistic models of materials were used in the calculations. The presence of a gap, as well as the sinusoidal nature of the heat dissipation power, leads to the fact that only a part of the surfaces of the fuel pellets comes into contact with the cladding. The results of the calculations showed that considering the creep effect made it possible to reduce the stress level in the fuel pellets and cladding several times.

References

[1] P. Aronov, M. Galanin, and A. Rodin. Numerical solution to the contact interaction problem of nuclear fuel element components using the mortar method and the domain decomposition method. *Herald of the Bauman Moscow State Technical University, Series Natural Sciences*, 96(3):4–22, 2021.

[2] P. Aronov, M. Galanin, and A. Rodin. Mathematical modeling of the contact interaction of the fuel element section, including up to 100 pellets, taking into account creep. *WSEAS Transactions on Applied and Theoretical Mechanics*, 17:71–78, 2022.

[3] P. Aronov, M. Galanin, and A. Rodin. Mathematical modeling of contact interaction of fuel elements with considering the creep using the mortar method. *AIP Conference Proceedings*, 2549:210008, 2023.

[4] I. M. Babuška. The finite element method with penalty. *Mathematics of Computation*, 27:221–228, 1973.

[5] O. Dahlblom and N. S. Ottosen. Smeared crack analysis using generalized fictitious crack model. *Journal of Engineering Mechanics*, 116(1):55–76, 1990.

[6] C. Eck and B. Wohlmuth. Convergence of a contact-neumann iteration for the solution of two-body contact problems. *Mathematical Models and Methods in Applied Sciences*, 13:1103–1118, 2003.

[7] M. Galanin and A. Rodin. Modeling a fuel element using the domain decomposition method. *AIP Conference Proceedings*, 2448:020007, 2021.

[8] M. Galanin and A. Rodin. Investigation and application of the domain decomposition method for simulating fuel elements. *Computational Mathematics and Mathematical Physics*, 62:641–657, 2022.

[9] M. Galanin and A. Rodin. Solution to a coupled problem of thermomechanical contact of fuel cell elements. *Journal of Applied Mechanics and Technical Physics*, 65(2):99–109, 2024.

[10] D.L. Hargman. *A Library of Materials Properties for Use in the analysis of Light Water Reactor Fuel Rod Behavior*. NUREG/CR-6150 TREE-1280, 1993.

[11] I. Huněk. On a penalty formulation for contact-impact problems. *Computers & Structures*, 48(2):193–203, 1993.

[12] S. Korobejnikov. *Nonlinear Deformation of Solids*. SB RAS, Novosibirsk, 2000.

[13] N. Malinin. *Applied Theory of Plasticity and Creep*. Mechanical engineering, Moscow, 1975.

[14] L. Rozin. *Variational Problem Statements for Elastic Systems*. Leningrad University, Leningrad, 1978.

[15] M. Suzuki and H. Saitou. *Water Reactor Fuel Analysis Code FEMAXI-6. Detailed Structure and User's Manual*. Japan Atomic Energy Agency, 2006.

[16] A. Toselli and O. B. Widlund. *Domain Decomposition methods — Algorithms and Theory*. Speinger-Verlag, Berlin-Heidelberg, 2005.

[17] B. Wohlmuth. A mortar finite element method using dual spaces for the lagrange multiplier. *SIAM Journal on Numerical analysis*, 38:989–1012, 2000.

[18] B. Wohlmuth. Variationally consistent discretization schemes and numerical algorithms for contact problems. *Acta Numerica*, 20:569–734, 2011.

[19] P. Wriggers. *Computational Contact Mechanics*. Speinger-Verlag, Berlin-Heidelberg, 2006.

[20] V. Zarubin and G. Kuvyrkin. *Mathematical Models of Continuum Mechanics and Electrodynamics*. Bauman Moscow State Technical University, Moscow, 2008.